

1 **Uncertainty analysis of eddy covariance CO₂ flux**
2 **measurements for different EC tower distances using an**
3 **extended two-tower approach**

4 **H. Post¹, H.J. Hendricks Franssen¹, A.Graf¹, M. Schmidt¹, H. Vereecken¹**

5 [1] {Agrosphere (IBG-3), Forschungszentrum Jülich GmbH, 52425 Jülich, Germany}

6

7 **Abstract**

8 The use of eddy covariance CO₂ flux measurements in data assimilation and other
9 applications requires an estimate of the random uncertainty. In previous studies, the
10 (classical) two-tower approach has yielded robust uncertainty estimates, but care must be
11 taken to meet the often competing requirements of statistical independence (non-overlapping
12 footprints) and ecosystem homogeneity when choosing an appropriate tower distance. The
13 role of the tower distance was investigated with help of a roving station separated between 8
14 m and 34 km from a permanent EC grassland station. Random uncertainty was estimated for
15 five separation distances with the classical two-tower approach and an extended approach
16 which removed systematic differences of CO₂ fluxes measured at two EC towers. This
17 analysis was made for a dataset where (i) only similar weather conditions at the two sites
18 were included, and (ii) an unfiltered one. The extended approach, applied to weather-filtered
19 data for separation distances of 95 m and 173 m gave uncertainty estimates in best
20 correspondence with an independent reference method. The introduced correction for
21 systematic flux differences considerably reduced the overestimation of the two-tower based
22 uncertainty of net CO₂ flux measurements and decreased the sensitivity of results to tower
23 distance. We therefore conclude that corrections for systematic flux differences (e.g. caused
24 by different environmental conditions at both EC towers) can help to apply the two-tower
25 approach to more site pairs with less ideal conditions.

26 **Keywords:** Eddy covariance, measurement uncertainty, random error, NEE, footprint,
27 systematic flux differences

28 **1 Introduction**

29 The net ecosystem exchange of CO₂ between the land surface and the atmosphere (*NEE*) can
30 be determined with the eddy covariance (EC) method. *NEE* is positive if the amount of CO₂
31 released to the atmosphere via respiration is higher than the amount of CO₂ assimilated
32 during photosynthesis. In contrast, negative *NEE* values denote a higher CO₂ uptake and a net
33 flux from the atmosphere into the ecosystem. During night-time, *NEE* is mainly a function of
34 respiration and therefore positive fluxes predominate, whereas during (summer) daytime
35 negative *NEE* values predominate because more CO₂ is assimilated than respired. Eddy
36 covariance CO₂ flux measurements are commonly used to analyze the interactions between
37 terrestrial ecosystems and the atmosphere which is crucial for the understanding of climate-
38 ecosystem feedbacks. In this regard reliable EC data with appropriate uncertainty estimates
39 are crucial for many application fields, such as the evaluation and improvement of land
40 surface models (e.g. Braswell et al., 2005; Hill et al., 2012; Kuppel et al., 2012).

41 When using the term ‘uncertainty’, we here focus on the random error following the
42 definition in Dragoni et al. (2007). It differs from the systematic error in that it is
43 unpredictable and impossible to correct (but can be quantified). Uncertainty doesn’t
44 accumulate linearly but “averages out” and can be characterized by probability distribution
45 functions (Richardson et al., 2012). Systematic errors are considered to remain constant for a
46 longer time period (> several hours). Ideally they can be corrected, but in case of EC
47 measurements this is still limited by either our understanding of various error sources or
48 insufficient background data. Systematic errors arise not only from instrumental calibration
49 and data processing deficits, but also from unmet underlying assumptions about the
50 meteorological conditions (Richardson et al., 2012). A main assumption is that turbulence is
51 always well developed in the lowest atmospheric boundary layer and responsible for the mass

52 transport while horizontal divergence of flow and advection are assumed to be negligible
53 (Baldocchi, 2001). Moreover, the EC method is based on the mass conservation principle,
54 which requires the assumption of steady state conditions of the meteorological variables
55 (Baldocchi, 2003). In case of CO₂ fluxes, night-time respiration is often underestimated due
56 to low wind velocities conditions and a temperature inversion which hinders the upward
57 carbon dioxide transport (Baldocchi, 2001). Hence, night-time data are commonly rejected
58 for further analysis (Barr et al., 2006).

59 After a possible correction of the EC flux data for systematic errors a random error will
60 remain which can arise from different sources such as (a) the assumption of a constant
61 footprint area within a measurement interval and the negligence of flux footprint
62 heterogeneity (e.g. due to temporal variability of wind direction, wind speed and atmospheric
63 stability which cause temporal variations of the footprint area); (b) turbulence sampling errors
64 which are related to the fact that turbulence is a highly stochastic process and especially the
65 sampling or not sampling of larger eddies is associated with considerable random fluctuations
66 of fluxes, even if they are already averaged over a 30-minutes period; and (c) instrumentation
67 deficits that can e.g. cause random errors in the measured variables (such as the CO₂ mixing
68 ratio and the vertical wind velocity) used to calculate the net CO₂ flux (Aubinet et al., 2011,
69 p. 179; Flanagan and Johnson, 2005).

70 Within the past decade, several approaches have been proposed to quantify the uncertainty of
71 eddy covariance CO₂ flux measurements. With the “two-tower” or “paired tower” approach
72 simultaneous flux measurements of two EC towers are analyzed (Hollinger et al., 2004;
73 Hollinger and Richardson, 2005). For the uncertainty quantification with the two-tower
74 approach, it is necessary that environmental conditions for both towers are nearly identical
75 (Hollinger et al., 2004; Hollinger and Richardson, 2005). However, most eddy covariance

76 sites do not have a nearby second EC tower to provide nearly identical environmental
77 conditions. Therefore, Richardson et al. (2006) introduced the “one-tower” or “24-h
78 differencing” method which is based on the two-tower approach. The main difference is that
79 the uncertainty estimate is based on differences between fluxes measured on subsequent days
80 if environmental conditions were similar on both days. Because most often environmental
81 conditions are not the same on two subsequent days (Liu et al., 2006), the applicability of this
82 method suffers from a lack of data and the random error is overestimated (Dragoni et al.,
83 2007). The model residual approach (Dragoni et al., 2007; Hollinger and Richardson, 2005;
84 Richardson et al., 2008) calculates CO₂ fluxes with a simple model and compares calculated
85 values with measured values. The model residual is attributed to the random measurement
86 error. The method is based on the assumption that the model error is negligible, which is
87 however a very questionable assumption. Alternatively, if the high-frequency raw-data of an
88 EC tower are available, uncertainty can be estimated directly from their statistical properties
89 (Billesbach, 2011). Finkelstein and Sims (2001) introduced an operational quantification of
90 the instrumental noise and the stochastic error by calculating the auto- and cross-covariances
91 of the measured fluxes. This method was implemented into a standard EC data processing
92 scheme by Mauder et al. (2013). The advantage is that a second tower or the utilization of
93 additional tools such as a simple model to estimate the EC measurement uncertainty is no
94 longer required. However, many data users do not have access to the raw-data but to
95 processed EC data only. Moreover, a large amount of solid metadata about the setup of the
96 EC measurement devices is required (but often not provided at second hand) to obtain
97 reliable raw-data based uncertainty estimates adequately. Therefore a two-tower based
98 approach has still a large group of users. In particular with regard to pairs of nearby towers
99 from local clusters which play an increasing role in the monitoring strategies of e.g. ICOS
100 and NEON, and have already been employed in case studies (e.g. Ammann et al., 2007).

101 Important advantages of the two-tower approach are (1) its simplicity and user friendliness,
102 (2) its usability for relatively short non gap-filled time series of several months, and (3) the
103 independence of a model.

104 The classical two-tower approach (Hollinger et al., 2004; Hollinger and Richardson, 2005;
105 Richardson et al., 2006) is based on the assumption that environmental conditions for both
106 EC towers are identical and flux footprints should not overlap to guarantee statistical
107 independence. Hollinger and Richardson (2005) use threshold values for three variables
108 (photosynthetically active photon flux density PPF, temperature & wind speed) to
109 determine whether environmental conditions are equivalent. Independent of this definition,
110 our understanding of “environmental conditions” includes both weather conditions and land
111 surface properties such as soil properties (texture, density, moisture, etc.), plant
112 characteristics (types, height, density, rooting depth, etc.), nutrient availability and fauna
113 (rabbits, earthworms, microorganisms, etc.), which are irregularly distributed and affect
114 respiration and/or photosynthesis. Strictly speaking, if footprints do not overlap 100%, the
115 assumption of identical environmental conditions is already not fulfilled. When applying a
116 two-tower based approach it is important to assure that systematic differences of the
117 measured fluxes, which are partly caused by within site or among site heterogeneity, are not
118 attributed to the random error estimate of the measured *NEE*. Our assumption that even
119 within a site with apparently one uniformly distributed vegetation type (and for very short EC
120 tower distances) land surface heterogeneity can cause significant spatial and temporal
121 variability in measured *NEE* is e.g. supported by Oren et al. (2006). They found that the
122 spatial variability of ecosystem activity (plants and decomposers) and LAI within a uniform
123 pine plantation contributes to about half of the uncertainty in annual eddy covariance *NEE*
124 measurements while the other half is attributed to micrometeorological and statistical
125 sampling errors. This elucidates the relevance of considering systematic flux differences

126 caused by within site ecosystem heterogeneity when calculating a two-tower based
127 uncertainty estimate.

128 Given the fact that site specific, adequate uncertainty estimates for eddy covariance data are
129 very important but still often neglected due to a lack of resources, we are aiming to advance
130 the two-tower approach so that it can also be applied if environmental conditions at both eddy
131 covariance towers are not very similar.

132 The main objectives of this study were (1) to analyze the effect of the EC tower distance on
133 the two-tower based CO₂ flux measurement uncertainty estimate and (2) to extend the two-
134 tower approach with a simple correction term that removes systematic differences in CO₂
135 fluxes measured at the two sites. This extension follows the idea of the extended two-tower
136 approach for the uncertainty estimation of energy fluxes presented in Kessomkiat et al.
137 (2013). The correction step is important for providing a more reliable random error estimate.
138 In correspondence with these objectives we analyzed the following questions: What is an
139 appropriate EC tower distance to get a reliable two-tower based uncertainty estimate? Can the
140 random error be quantified in reasonable manner with the extended two-tower approach, even
141 though environmental conditions at both EC towers are clearly not identical? The total
142 random error estimated with the raw-data based method (Mauder et al., 2013) was used as a
143 reference to evaluate our extended two-tower approach based results.

144 **2 Test sites and EC Tower setup**

145 The Rollesbroich test site is an extensively used grassland site, located in the Eifel region of
146 western Germany (Fig.1). The mean temperature in Rollesbroich is ~ 7.7°C and the mean
147 precipitation is ~ 1033mm per year (Korres et al., 2010). Predominating soil types at the site
148 are Cambisols with a high clay and silt content (Arbeitsgruppe BK50, 2001). The grass

149 species grown in Rollesbroich are mainly ryegrass, particularly perennial ryegrass (*lolium*
150 *perenne*), and smooth meadow grass (*poa pratensis*) (Korres et al., 2010). A permanent eddy
151 covariance tower (EC1) is installed at the Rollesbroich site since May 2011 at a fixed
152 position. The measurement height of the sonic anemometer (CSAT3, Campbell Scientific,
153 Logan, UT, U.S.A.) and the open-path gas analyzer (Li7500, Li-Cor, Lincoln, NE, U.S.A.) is
154 2.6 m above ground. The canopy height was measured every 1-2 weeks and varied between
155 0.03 m and 0.88 m during the measurement period. A second EC tower, the roving station
156 (EC2), has been installed at four different distances (8 m, 95 m, 173 m and 20.5 km) from
157 EC1 for time periods ranging between 3 and 7.5 months (Tab.1). The EC2 location “Kall-
158 Sistig” 20.5 km north-east of Rollesbroich is another grassland site with similar
159 environmental conditions as Rollesbroich. The vegetation in Kall-Sistig is extensively
160 managed C3 grass, the same as for Rollesbroich. However, the average plant height measured
161 between Aug. 14th and Oct. 30th 2012 was lower (~ 0.15 m) than the respective average for
162 Rollesbroich (~ 0.2 m), which is also true for the plant height measured in May and June
163 2012 (Kall-Sistig: ~ 0.22 m; Rollesbroich: ~ 0.29 m). As in Rollesbroich, clayey-silty
164 Cambisols are most widespread (Arbeitsgruppe BK50, 2001). The mean temperature for the
165 entire measurement interval in Kall-Sistig (Tab.1) measured at the EC station is 11.4 °C and
166 the soil moisture 32% compared to 11.0 °C and 35% in Rollesbroich (same time interval for
167 averaging). Additionally a third EC tower was located in Merzenhausen in ~ 34 km distance
168 to EC1 (Fig.1). Merzenhausen (MH) is an agricultural site, where winter wheat was grown
169 during the measurement period. Both the land use conditions and the average weather
170 conditions differ from those in Rollesbroich and Kall-Sistig. The climate at the lowland site
171 Merzenhausen is comparable to the one in Selhausen at a distance of 13 km from
172 Merzenhausen, where the mean precipitation is ~ 690 mm/a and the yearly mean temperature
173 ~9.8°C (Korres et al., 2010). The soils are mainly Luvisols with some patches of Kolluvisols

174 (Arbeitsgruppe BK50, 2001). The measurement devices of EC2 and EC3 are the same as the
175 EC1 devices and were installed 2.6 m above ground as well. Both, the sonic anemometers
176 and the open-path gas analyzers have been calibrated every 1-3 months thoroughly and
177 consistently. Details on the EC data acquisition are summarized in Sect. 3.1.

178 Rollesbroich is part of the TERENO network (Zacharias et al., 2011). Information and
179 additional data were collected showing that land surface properties are spatially
180 heterogeneous distributed at the Rollesbroich site: (1) Single fields at the Rollesbroich site
181 are managed by different farmers. Information the land owners provided, as well as periodic
182 camera shots and grass height measurements around the EC towers indicated that the timing
183 of fertilization and grass cutting as well as the amount of manure applied varied between the
184 single fields during the measurement period; (2) Soil type distribution as displayed in the
185 German soil map shows heterogeneity (Arbeitsgruppe BK50, 2001); (3) Soil carbon and
186 nitrogen pools [g/kg] as well as bulk density [g/cm³] and content of rock fragments [%]
187 measured from April-May 2011 in three soils horizons at 94 locations across the Rollesbroich
188 site are spatially highly variable (H. Schiedung 2013, personal communication); (4) During
189 the eddy covariance measurement period, soil moisture and soil temperature data were
190 collected in 10 min. resolution at three depths (5 cm, 20 cm and 50 cm) and 84 points by the
191 wireless sensor network (“SoilNet”; Bogena et al., 2009), calibrated for the Rollesbroich site
192 by Qu et al., (2013). SoilNet data shows that soil moisture is heterogeneously distributed
193 within the Rollesbroich site (Qu et al., 2014, submitted).

194 **3 Data and Methods**

195 **3.1. EC data processing**

196 The EC raw data were measured with a frequency of 20 Hz and fluxes were processed for
197 flux intervals of 30 minutes. The complete processing of the data was performed with the
198 TK3.1 software (Bayreuth, Department of Micrometeorology, Germany; Mauder and Foken,
199 2011), using the standardized strategy for EC data calculation and quality assurance
200 presented in detail by Mauder et al., 2013. The strategy includes established EC conversions
201 and corrections such as e.g. correction of spectral loss (Moore, 1986) and correction for
202 density fluctuations (Webb et al., 1980). It includes tests on high frequency data (site specific
203 plausibility limits, statistical spike detection) as well as on processed half hourly fluxes such
204 as stationarity and integral turbulence tests (Foken and Wichura, 1996). The tests on half
205 hourly fluxes are the basis for a standardized quality flagging according to Foken et al. (2004)
206 that classifies flux measurements as high (0), moderate (1) or low (2) quality data. For this
207 analysis only flux measurements assigned to 0 or 1 were used, while low quality data were
208 treated as missing values. Besides quality flags TK3.1 also provides footprint estimates
209 (Kormann and Meixner, 2001) and uncertainty estimates that were used for interpreting and
210 analyzing flux data. To avoid introduction of additional uncertainty no gap filling of flux time
211 series was performed.

212 **3.2. Uncertainty estimation based on the two-tower approach**

213 The two-tower approach (Hollinger et al., 2004; Hollinger and Richardson, 2005; Richardson
214 et al., 2006) defines the random error of *NEE* eddy covariance measurements as the standard
215 deviation $\sigma(\delta)$ of the difference between the CO₂ fluxes [$\mu\text{mol m}^{-2}\text{s}^{-1}$] simultaneously
216 measured at two different EC towers (NEE_1, NEE_2):

$$\sigma(\delta) = \frac{\sigma (NEE_1 - NEE_2)}{\sqrt{2}} \quad \text{Eq. 1}$$

217 Based on Eq.1 we calculated the two-tower based uncertainty estimates using the NEE_1 data
 218 measured at the permanent EC tower in Rollesbroich (EC1) and the NEE_2 data of a second
 219 tower which was either the roving station (EC2) or – in case of the 34 km EC tower distance
 220 – another permanent EC tower (EC3, Tab.1).

221 For comparison, the measurement uncertainty $\sigma(\delta)$ was calculated separately for each EC
 222 tower distance (Tab.1) and independently for each of the following schemes:

- 223 1. The classical two-tower approach (Hollinger et al., 2004; Hollinger and Richardson,
 224 2005; Richardson et al., 2006).
- 225 2. The classical two-tower approach including a filter for similar weather conditions
 226 (Sect. 3.4).
- 227 3. The extended two-tower approach with an added correction for systematic flux
 228 differences (sfd-correction; Sect. 3.3), without weather-filter.
- 229 4. The extended two-tower approach with sfd-correction and the previously applied
 230 weather-filter.

231 The uncertainty estimate of the two-tower approach is obtained by dividing the NEE data
 232 series into several groups (“bins”) according to the flux magnitude and then using Eq. 1 to
 233 calculate the standard deviation $\sigma(\delta)$ for each group (Richardson et al., 2006). Finally, a
 234 linear regression function between the flux magnitude and the standard deviation can be
 235 derived. The linear correlation of the uncertainty and the flux magnitude can be explained by
 236 the fact that the flux magnitude is a main driving factor for the random error and can explain
 237 about 63% of the variance in the CO_2 flux error as shown in a case study by Richardson et al.

238 (2006). Accordingly, we calculated the standard deviation $\sigma(\delta)$ [$\mu\text{mol m}^{-2} \text{s}^{-1}$] based on 12
239 groups of the CO_2 flux magnitude; six groups for positive and six groups for negative fluxes.
240 Fixed class limits for the flux magnitude would have led to a different number of samples in
241 each group. Now class limits were set such that all groups with positive NEE values had an
242 equal amount of half hourly data, the same holds for all groups with negative NEE values.
243 For each single group the standard deviation $\sigma(\delta)$ was calculated using the single half-hourly
244 flux differences of NEE_1 and NEE_2 . The corresponding mean NEE magnitude for each group
245 member was determined by averaging all half-hourly means of NEE_1 and NEE_2 in the
246 respective group. Then, the linear regression equation was derived separately for negative and
247 positive NEE values using the 6 calculated standard deviations $\sigma(\delta)$ and the 6 mean NEE
248 values. This procedure was carried out for each dataset of the five EC tower distances and
249 again for each of the four uncertainty estimation schemes so that altogether 20x2 linear
250 regression equations were derived. The significance of the correlation between the NEE
251 magnitudes and the standard deviations $\sigma(\delta)$ was tested with the p -value determined with the
252 Student's t-test based on Pearson's product moment correlation coefficient r . Moreover, the
253 95% confidence intervals of the slope and the intercept for each linear regression equation
254 were determined. The linear regression equations were calculated imposing as constraint an
255 intercept ≥ 0 , because a negative standard deviation is not possible. With those linear
256 regression equations, the uncertainty for the individual half-hourly NEE measurement values
257 of the permanent EC tower in Rollesbroich (EC1) were estimated using the individual half-
258 hourly NEE_1 values [$\mu\text{mol m}^{-2} \text{s}^{-1}$] as input (x) to calculate the corresponding uncertainty
259 $\sigma(\delta)$ [$\mu\text{mol m}^{-2} \text{s}^{-1}$] (y).

260 The described calculation of the individual NEE uncertainty values was done for all half
261 hourly NEE data, including those data points that were discarded by the weather filter

262 (Sect.3.4) and/or the sfd-correction (Sect.3.3). Hence, for each of the four two-tower based
263 uncertainty estimation schemes the same amount of individual *NEE* uncertainty values was
264 generated. These mean uncertainty estimates were used to evaluate the effect of the EC tower
265 distance as well as the sfd-correction and the weather-filter on the two-tower based
266 uncertainty estimation. Even though Hollinger et al. (2004) and Richardson and Hollinger
267 (2005) already pointed out that the two-tower approach assumes similar environmental
268 conditions and non-overlapping footprints, we applied the classical approach for all EC tower
269 distances, even if these basic assumptions were not fulfilled, to allow for a comparison of the
270 results before and after the usage of the weather-filter and the sfd-correction (extended two-
271 tower approach).

272 **3.3. Correction for systematic flux differences (sfd-correction)**

273 Different environmental conditions and other factors such as instrumental calibration errors
274 can cause systematic flux differences between two towers. Because these flux differences are
275 not inherent to the actual random error of the measured *NEE* at one EC tower station they
276 lead to an overestimation of the two-tower approach based uncertainty. Therefore, we
277 extended the classical two-tower approach with a simple correction step for systematic flux
278 differences (sfd-correction). The reason why systematic flux differences can statistically be
279 separated quite easily from random differences of the EC flux measurements is their
280 fundamentally different behavior in time: random differences fluctuate highly in time
281 whereas systematic differences tend to be constant over time or vary slowly. The sfd-
282 correction introduced is similar to the second correction step in Kessomkiat et al. (2013,
283 Equation 6 therein), but adapted to the measured *NEE* instead of latent and sensible heat
284 fluxes. An averaging time interval of 12 hours was used to calculate the running mean for the
285 sfd-correction. For each moving average interval, the mean NEE_{12h} of one EC tower

286 (separately for EC1 and EC2) [$\mu\text{mol m}^{-2} \text{s}^{-1}$] and the mean CO_2 flux averaged over both EC
287 towers NEE_{2T_12h} [$\mu\text{mol m}^{-2} \text{s}^{-1}$] were calculated to define the sfd-correction term which was
288 used to calculate the corrected NEE_{corr} [$\mu\text{mol m}^{-2} \text{s}^{-1}$]:

$$NEE_{corr} = \frac{NEE_{2T_12hr}}{NEE_{12h}} \cdot NEE \quad \text{Eq. 2}$$

289 NEE is the single half-hourly, processed NEE value [$\mu\text{mol m}^{-2} \text{s}^{-1}$] of one EC tower. Only if
290 both NEE data, NEE_{-EC1} - for the permanent EC1 tower and NEE_{-EC2} - for the second tower,
291 were available at a particular half hourly time step and if both values were either positive or
292 negative, the respective data were included to calculate the correction term. The running
293 averages were only calculated if at least 50% of the data for NEE_{-EC1} - and NEE_{-EC2} remained
294 for averaging in that particular window. Due to the frequent occurrence of gaps in the data
295 series the amount of available NEE_{corr} values considerably decreased by applying stricter
296 criteria like 70% or 90% data availability (Tab. A2). We assume a 12 hour averaging period
297 to be long enough to exclude most of the random error part but short enough to consider daily
298 changes of systematic flux differences. For a six hour interval for instance the uncertainty of
299 the mean NEE is usually higher. For larger window sizes (24 or 48 hours) further analysis
300 was hampered by too many data gaps, i.e. the 50% criterion was hardly ever fulfilled and not
301 enough averages remained to allow for the two-tower based uncertainty estimation (Tab. A2).
302 The correction was done separately for positive and negative fluxes, due to the different
303 sources, properties and magnitudes of the CO_2 flux measurements and different errors for
304 daytime (negative) and night-time (positive) fluxes (e.g. Goulden et al., 1996; Oren et al.,
305 2006; Wilson et al., 2002).

306 The final sfd-corrected $NEE1_{corr}$ values for EC1 and $NEE2_{corr}$ values for EC2 should not be
307 understood as corrected NEE flux data. They were used only to enhance the two-tower based

308 uncertainty estimation in a way that systematic flux differences which cause an
309 overestimation of the uncertainty are filtered out. Moreover, systematic flux differences at
310 two EC towers are not to be confused with systematic errors, which are independent of the
311 uncertainty estimation method and optimally corrected before the random error is estimated.

312 **3.4. Filter for weather conditions**

313 For larger distances of two EC towers, such as the 20.5 km and 34 km distance in this study,
314 different weather conditions can cause differences of the measured fluxes in addition to the
315 different land surface properties. Some weather variables (e.g. temperature) are following a
316 clear diurnal and annual course and differences in e.g. temperature at two EC towers are
317 therefore relatively constant. This is expected to cause rather systematic differences in the
318 measured *NEE* which can be captured with the sfd-correction. However, other variables such
319 as wind speed or incoming short wave radiation are spatially and temporally much more
320 variable, for example related to single wind gusts or cloud movement. Differences in the
321 measured fluxes at two EC towers caused by those spatial-temporally highly variable weather
322 variables cannot be captured well with the sfd-correction term due to this “random character”.
323 However, a weather filter can account for this because it compares the differences in weather
324 variables at each single time step. Therefore a filter for similar weather conditions was
325 applied in addition to the sfd-correction following Hill et al. (2012) and Richardson et al.
326 (2006) to only include half hourly *NEE* data, if the weather conditions at the second EC tower
327 are similar to those at the permanent EC1 tower location in Rollesbroich. Following the
328 definition in Richardson et al. (2006), similar weather conditions were defined by a
329 temperature difference $< 3^{\circ}\text{C}$; wind speed difference $< 1 \text{ m/s}$ and difference in PPFD < 75
330 $\mu\text{mol m}^{-2} \text{ s}^{-1}$. The weather-filter was applied before the (classical) uncertainty estimation and
331 the sfd-correction. As shown e.g. in Tsubo and Walker (2005), the incoming short wave

332 radiation (or solar irradiance SI) and the photosynthetically active radiation (PAR) are
333 linearly correlated. Accordingly SI and PPF measured at the EC1 station in Rollesbroich
334 were also linearly correlated. Because direct PPF measurements were not available for all
335 measurement periods, we derived a linear regression equation on the basis of all SI and PPF
336 data for the permanent EC tower station (EC1). Using this equation, missing PPF values
337 were estimated if only SI but no PPF data were available at a certain time step.

338 **3.5. Footprint analysis**

339 The footprint analysis was applied to quantify the percentage footprint overlap of the two EC-
340 stations during the measurement periods. This information was not used to filter the data but
341 to allow for a better understanding of the mean uncertainty estimates for the different
342 scenarios. Using the analytical model of Kormann and Meixner (2001) implemented in the
343 TK3.1 software (Mauder and Foken, 2011), a grid of estimated source weights (resolution 2
344 m, extension 1 km by 1 km) was computed for each half-hour and station position. The
345 overlap between the footprints of two simultaneously measuring towers was then quantified
346 as:

$$O_{12}(t) = \sum_{x=1}^N \sum_{y=1}^M \min(f_1(x, y, t), f_2(x, y, t)) \quad \text{Eq. 3}$$

347 The indices 1 and 2 indicate the tower and t the time (in our case, half-hour). N and M are the
348 number of pixels in east-west and north-south direction, x and y the respective running
349 indices. The minimum function $\min()$ includes the source weight f computed for the
350 respective tower, x and y location, and half-hour. O is 1 if both source weight grids are
351 identical, and 0 in case of no overlap. During stable conditions, the footprint area of a tower
352 increases and can result in considerable source weight contributions from outside the

353 modeling domain. Assuming that two footprints which overlap highly in the modeling
 354 domain likely continue to overlap outside the modeling domain, O as defined above might be
 355 low-biased in such cases. We therefore additionally considered a normalized version
 356 $O/\min(\Sigma\Sigma f_i, \Sigma\Sigma f_i)$ as an upper limit estimate of the overlap. The overlap for the additional
 357 sites Kall and Merzenhausen more than 20 km away was assumed zero.

358 **3.6. Comparison measures**

359 To compare and evaluate the two-tower based uncertainty estimates, we calculated random
 360 error estimates based on Mauder et al. (2013) as a reference. This reference method is
 361 independent of the two-tower based approach, because data of only one EC tower are used to
 362 quantify the random error of the measured fluxes and raw data instead of the processed fluxes
 363 are used. The raw-data based random error estimates – the instrumental noise σ_{cov}^{noise} and the
 364 stochastic error σ_{cov}^{stoch} – were calculated independently. Mauder et al. (2013) determine the
 365 instrumental noise based on signal autocorrelation. Following Finkelstein and Sims (2001)
 366 the stochastic error is calculated as the statistical variance of the covariance of the flux
 367 observations. Generally, σ_{cov}^{noise} was considerably lower than σ_{cov}^{stoch} . The total raw-data based
 368 random error σ_{cov} [$\mu\text{mol m}^{-2}\text{s}^{-1}$] was calculated by adding σ_{cov}^{noise} and σ_{cov}^{stoch} “in quadrature”

369 ($\sigma_{cov} = \sqrt{\sigma_{cov}^{stoch^2} + \sigma_{cov}^{noise^2}}$) according to Aubinet et al. (2011, p.176). The mean reference
 370 σ_{cov} used for the evaluation of the two-tower based random error estimates was calculated
 371 by averaging the single half-hourly σ_{cov} values for the permanent EC1 tower in Rollesbroich.
 372 In order to be consistent with the two-tower based calculations, exactly the same half hourly
 373 time steps of the EC1 data series used for the two-tower based uncertainty estimation were
 374 used to calculate the corresponding mean reference values σ_{cov} . As indicator for the
 375 performance of the two-tower based uncertainty estimation schemes applied for the five

376 different EC tower distances, the relative difference $\Delta \sigma_{cov}$ [%] of a two-tower based
377 uncertainty value [$\mu\text{mol m}^{-2} \text{s}^{-1}$] and σ_{cov} [$\mu\text{mol m}^{-2} \text{s}^{-1}$] was calculated:

$$\Delta\sigma_{cov}[\%] = \frac{\sigma(\delta) - \sigma_{cov}}{\sigma_{cov}} * 100 \quad \text{Eq. 4}$$

378 Then, $\Delta \sigma_{cov}$ values were compared for the different EC tower separation distances and two-
379 tower based uncertainty estimation schemes. The performance of the two-tower based
380 uncertainty estimation was considered better if σ_{cov} [%] was closer to zero.

381

382 **4 Results**

383 **4.1. Classical two-tower based random error estimates**

384 Fig.2 and Fig.3 show the linear regressions of the random error $\sigma(\delta)$ (also referred to as
385 “standard error” or “uncertainty”) as function of the *NEE* magnitude according to the
386 classical two-tower approach for the different EC tower distances without weather-filter
387 (Fig.2) and with weather-filter (Fig.3). The dashed linear regression lines denote that the
388 linear correlation between $\sigma(\delta)$ and *NEE* is weak ($p > 0.1$), which is in particular true for the
389 positive *NEE* values measured for 173 m and 20.5 km EC tower distances as well as for the
390 negative *NEE* values for 20.5 km and 34 km distance. The 95% confidence intervals of the
391 respective slopes and the intercepts are summarized in the Appendix (Tab.A1). Uncertainty
392 estimation with the classical two-tower approach is critical for those larger distances because
393 measured flux differences caused by different environmental conditions at both EC towers
394 can superimpose the random error signal which e.g. originates from instrumental or
395 turbulence sampling errors. This weakens the correlation of the random error and the flux

396 magnitude. This is not surprising since Hollinger et al. (2004) and Richardson and Hollinger
397 (2005) already pointed out that similar environmental conditions are a basic assumption of
398 the two-tower approach. Therefore, statements of how the weather filter affects the mean
399 uncertainty estimate $\sigma(\delta)$ for those large distances need to be treated with caution.

400 The weather-filtering only increased the correlation between the flux magnitude and the
401 random error $\sigma(\delta)$ for positive fluxes for separation distances of 173 m and 20 km whereas in
402 most cases the linear correlation was weakened, mainly due to a decreased number of
403 samples in each averaging group of the *NEE* flux magnitude. Therefore, testing stricter
404 weather-filter criteria (e.g. wind speed < 0.5 m/s, PPFD < 50 $\mu\text{mol m}^{-2} \text{s}^{-1}$, Temp < 2 °C),
405 which caused a decline of samples in each group from e.g. $n > 1000$ to 24 or less, resulted in
406 little meaningful results.

407 As illustrated in Tab.2, the mean *NEE* uncertainty estimate based on the classical two-tower
408 approach increased as a function of EC tower distance. However, without applying the
409 weather-filter, the mean uncertainty $\sigma(\delta)$ was nearly identical for the two largest distances
410 (20.5 km and 34 km), although e.g. the land cover and management in Merzenhausen (EC3
411 tower at 34 km separation) were different from the Rollesbroich site. As a result of the
412 weather-filtering, the mean uncertainty was less overestimated for the distances 173m and
413 20.5 km. However, for the 95 m and 34 km distance, the overestimation of the uncertainty
414 estimate increased by the weather-filtering (Tab.2). This implies that for the classical two-
415 tower approach (without sfd-correction) weather-filtering did not clearly reduce the
416 overestimation of the uncertainty for largest EC tower distances (20.5 km and 34 km) where
417 weather-filtering is expected to be particularly relevant.

418 Comparing the mean uncertainty estimates of the classical two-tower approach with the
419 reference random error estimates σ_{cov} , indicates that both with and without weather filter the
420 uncertainties were overestimated (Tab.2), for all EC tower differences. This could be
421 expected for the large distances, because basic assumptions for the application of the classical
422 two-tower approach are violated for these large distances. But results illustrate that even for
423 short EC tower distances *NEE* uncertainty estimated with the classical two-tower approach is
424 larger than the raw-data based estimates (Tab.2).

425 **4.2. Extended two-tower approach**

426 The scatter plots in Fig.4 illustrate the effect the sfd-correction (Eq.2) had on the difference
427 of the *NEE* data simultaneously measured at both EC towers (NEE_{-EC1-} and NEE_{-EC2-}). The
428 sfd-correction reduced the bias and scattering, because systematic differences of the
429 measured fluxes, e.g. induced by different environmental conditions, were removed. As
430 expected, the effect of the sfd-correction was considerably higher for the larger EC tower
431 distances because environmental conditions are also expected to differ more if the distance of
432 two locations is larger. For the 8 m EC tower distance for instance, the effect of the sfd-
433 correction is very minor because footprints are often nearly overlapping. However, for the EC
434 tower distances ≥ 173 m, the bias and scattering of NEE_{-EC1-} and NEE_{-EC2-} was considerably
435 reduced by the sfd-correction.

436 A comparison of Fig.2 and Fig.5 illustrates how the sfd-correction affected the linear
437 regression of the *NEE* standard error as function of *NEE* flux magnitude: The sfd-correction
438 considerably enhanced the correlation of NEE_{corr} and the standard error $\sigma(\delta)_{corr}$ for the EC
439 tower distances 20.5 km and 34 km from $R^2 \geq 0.15$ to $R^2 \geq 0.43$.

440 Applying the sfd-correction (without weather-filter) reduced the mean uncertainty value by
441 41.6% to 56.9% for the EC tower distances from 8m to 34 km. The relative differences $\Delta \sigma_{cov}$
442 indicate that the correction for systematic flux differences considerably improved the two-
443 tower based uncertainty estimate for the distances >8 m (Tab.2): The difference $\Delta \sigma_{cov}$ was
444 notably smaller ($< 56.8\%$) for all distances except the 8 m distance compared to $\Delta \sigma_{cov}$
445 determined with the classical two-tower approach ($< 274.7\%$). The most considerable
446 improvement was achieved for the 95 m EC tower distance and the 173 m distance.
447 Additional application of the weather-filter (Fig.6) on the sfd-corrected NEE_{corr} data reduced
448 the mean uncertainty estimate $\sigma(\delta)_{corr}$ by 23.3% and 2.9% for the 20.5 km and the 34 km EC
449 tower distance and reduced $\Delta \sigma_{cov}$ by 57.7% and 7.7%. The effect of the weather-filter on the
450 uncertainty estimates of the shorter EC tower distances was very minor (Tab.2). The
451 uncertainty estimates $\sigma(\delta)_{corr,f}$ determined with the extended two-tower approach agree best
452 with the independent reference values σ_{cov} for the EC tower distances 95m and 173 m,
453 suggesting that those distances were most suitable for the application of the extended two-
454 tower approach.

455 **4.3. Discussion**

456 The results show that the two-tower based uncertainty estimates (both classical and extended
457 two-tower approach) were smallest for the 8 m distance. This can be explained with the
458 results of the footprint analysis: While the average percentage footprint overlap is 13%
459 (normalized 19%) for the 95 m EC tower distance and only 4% (7%) for the 173m EC tower
460 distance, it is 68% (80%) for the 8 m EC tower distance. The stronger overlap of the 8 m
461 distance footprint areas is associated with a more frequent sampling of the same eddies. As a
462 consequence, part of the random error was not captured with the two-tower approach. If EC

463 towers are located very close to each other (< 10 m) and the footprint overlap approaches
464 100%, only instrumental errors and stochasticity related to sampling of small eddies will be
465 captured with the two-tower based uncertainty estimate. Because the EC measurements are
466 statistically not independent if the footprints are overlapping, the classical EC tower method
467 is not expected to give reliable uncertainty estimates for very short EC tower distances
468 (Hollinger et al., 2004; Hollinger and Richardson, 2005). However, without applying the sfd-
469 correction, the mean uncertainty estimate $\sigma(\delta)$ was higher than the raw-data based reference
470 value σ_{cov} which includes both the instrumental noise σ_{cov}^{noise} and the stochastic error σ_{cov}^{stoch} .
471 The raw-data based σ_{cov}^{noise} itself was only $0.04 \mu\text{mol m}^{-2} \text{s}^{-1}$ of $0.64 \mu\text{mol m}^{-2} \text{s}^{-1}$ for the
472 dataset of the 8 m EC tower distance. The mean uncertainty value derived with the extended
473 two-tower approach $\sigma(\delta)_{corr,f}$ for the same dataset was lower than $\sigma(\delta)$ but still considerably
474 higher than σ_{cov}^{noise} , suggesting that even at 8 m EC tower distance instrumentation errors were
475 only a minor part of the two-tower based uncertainty estimate. For the larger separation
476 distances 95 m or 173 m with notably less footprint overlap turbulence sampling errors are
477 almost fully accounted for by a two-tower approach. (It should be noted that forest stations,
478 with a typically larger aerodynamic measurement height and footprint size, will require larger
479 separation distances). However, different land surface properties and management are more
480 likely for the larger separation distances and can cause systematic flux differences that should
481 not be attributed to the random error estimate. As outlined in section 2, land surface
482 properties related to management (e.g. nutrient availability due to fertilization), soil properties
483 (bulk density, skeleton fraction), soil carbon-nitrogen pools, soil moisture and soil
484 temperature are heterogeneously distributed at the Rollesbroich site. The effect of soil
485 moisture, soil temperature and soil properties on CO_2 fluxes (respiration mainly) is well
486 known (e.g. Herbst et al., 2009; Flanagan and Johnson, 2005; Xu et al., 2004; Lloyd and
487 Taylor, 1994; Orchard and Cook, 1983) as well as the role of grassland management (e.g.

488 Allard et al., 2007). Results indicate that an overestimation of the two-tower based
489 uncertainty caused by different land surface properties in the footprint area of both EC towers
490 can be successfully filtered out by the extended approach. It should be noted that a shorter
491 moving average interval of the sfd-correction term (e.g. 6 hours instead of the applied 12
492 hours window; Tab.A2), results in slightly lower uncertainty estimates compared to the
493 reference. This can be explained by a possible “over-correction” of the *NEE* data related to a
494 too short moving average interval for calculating the sfd-correction term. It needs to be
495 emphasized that the estimated mean *NEE* values of the moving average intervals are
496 associated with uncertainty. As mentioned, the moving average interval should be long
497 enough to exclude random differences of the simultaneously measured fluxes but short
498 enough to limit the impact of non-stationary conditions. However, the 12hr running mean
499 *NEE1* and *NEE2* values (NEE_{12}) as well as the respective means of *NEE1* and *NEE2*
500 ($NEE_{2T,12}$) used to calculate NEE_{corr} (Eq.2) are uncertain because they still contain the
501 random error part which cannot be corrected or filtered out. This uncertainty in the mean is
502 expected to be higher for a shorter averaging interval such as 6 hours. Therefore, completely
503 correcting the difference in mean *NEE* slightly overcorrects systematic differences in *NEE*. In
504 general results were not very sensitive to different moving average sizes of the sfd-correction
505 term and data coverage percentages defined for this interval (Tab.A3).

506 It is expected that systematic differences in measured *NEE* caused by spatially variable land
507 surface properties are stronger during the night than during the day since they affect
508 respiration more directly than photosynthesis (see e.g. Oren et al., 2006). Moreover, during
509 night-time and/or winter (positive *NEE*), some conditions associated with lower EC data
510 quality such as low turbulence, strong stability, and liquid water in the gas analyzer path
511 prevail more often than in summer and/or daytime (negative *NEE*). The less severe cases of

512 such conditions are not always completely eliminated by the quality control. In time series of
513 eddy-covariance fluxes this typically shows up as implausible fluctuations of the flux during
514 calm nights. This is reflected by plots of *NEE* flux magnitude versus uncertainty (Fig.2-3;
515 Fig.5-6) showing higher uncertainties for positive compared to negative *NEE* data which
516 agrees with previous findings (e.g. Richardson et al., 2006).

517 At very large EC tower distances (20.5 km, 34 km) footprints were not overlapping and the
518 environmental conditions were considerably different; in particular for the EC tower setup
519 Rollesbroich/Merzenhausen with different land use (grassland/crop) and climate conditions.
520 For those distances, the relative difference $\Delta \sigma_{\text{cov}}$ between σ_{cov} and $\sigma(\delta)$ (classical two-tower
521 approach) was much larger than $\Delta \sigma_{\text{cov}}$ between σ_{cov} and $\sigma(\delta)_{\text{corr,f}}$ (extended two-tower
522 approach). $\Delta \sigma_{\text{cov}}$ was reduced by 85.7% for the 20.5km distance and 79.3% for the 34km if
523 both sfd-correction and weather filter were used. However, after applying the sfd-correction
524 and the weather-filtering, the mean uncertainty estimate was still higher than the raw-data
525 based reference value (Tab.2), suggesting that for these large EC tower distances the sfd-
526 correction and the weather-filter do not fully capture systematic flux differences and
527 uncertainty is still overestimated by the extended two-tower approach. This can have
528 different reasons. We assume the major reason is that the weather-filter is supposed to
529 capture all measured flux differences that can be attributed to different weather conditions at
530 both EC towers which cannot be captured with the sfd-correction. Applying stricter
531 thresholds could increase the efficiency of the weather filter but in our case the reduced
532 dataset was too small to allow further analysis. In general, the weather-filter did not improve
533 the uncertainty estimates as much as the sfd-correction. However, this does not imply that
534 differences in weather conditions are negligible when applying the extended two-tower
535 approach for larger EC tower distances. In fact the systematic part of measured EC flux

536 differences between both towers caused by (steady, systematic) among-site differences in
537 weather conditions were already partly captured with the sfd-correction. In contrast, such
538 systematic differences were difficult to capture with the weather-filter because much lower
539 thresholds would have been required.

540 The absolute corrected and weather-filtered uncertainty value $\sigma(\delta)_{\text{corr,f}}$ [$\mu\text{mol m}^{-2} \text{s}^{-1}$] was
541 slightly lower for the 34 km EC tower distance than for the 20.5 km EC tower distance
542 (Tab.2). The raw-data based reference σ_{cov} [$\mu\text{mol m}^{-2} \text{s}^{-1}$] however was also smaller for the 34
543 km dataset than for the 20.5 km dataset which can be related to the different lengths and
544 timing (i.e., different seasons) of the measurement periods for each of the five EC tower
545 distances: The roving station was moved from one distance to another within the entire
546 measurement period of ~ 27 months. During this entire time period of data collection, the
547 length and timing of the single measurement periods varied for the five EC tower separation
548 distances (Tab.1). This is not optimal because the random error is directly related to the flux
549 magnitude and the flux magnitude itself is directly related to the timing of the measurements.
550 Because in spring and summer flux magnitudes are higher, the random error is generally
551 higher as well (Richardson et al., 2006). To reduce this effect, we captured spring/summer as
552 well as autumn/winter months in each measurement period. However, the timing of the
553 measurements and the amount of data available were not the same for the five EC datasets. In
554 particular the permanent EC tower in Merzenhausen was measuring considerably longer (> 2
555 years) than the roving station did for the other four EC tower distances. Therefore,
556 differences of the mean uncertainty estimates for the five measurement periods were partly
557 independent of the EC tower distance. This effect gets obvious when looking at the mean
558 uncertainties σ_{cov} estimated with the reference method, which should be independent of the
559 distance but were also found to be different for each dataset of the five EC tower distances.

560 Against this background, statements about how EC tower distances affect the two-tower
561 based uncertainty estimate need to be treated with caution.

562 The *NEE* uncertainty $\sigma(\delta)_{\text{corr},f}$ estimated for the grassland site Rollesbroich agree well with
563 the *NEE* uncertainty values for grassland sites by Richardson et al. (2006), and also the
564 regression coefficients (Fig. 2-3; Fig.5-6, Tab. A1) do not show large differences. This can be
565 expected since Richardson et al. (2006) applied their method for a very well-suited tower pair
566 with low systematic differences, such that the classical approach and our extended approach
567 should approximately converge. However, identical results are unlikely because even for two
568 very similar neighboring sites some systematic differences occur. In addition, the random
569 error is expected to vary between sites (see e.g. Mauder et al., 2013) which is in part related
570 to instrumentation.

571 **5 Conclusions**

572 When estimating the uncertainty of eddy covariance net CO₂ flux (*NEE*) measurements with
573 a two-tower based approach it is important to consider that the basic assumptions of identical
574 environmental conditions (including weather conditions and land surface properties) on the
575 one hand and non-overlapping footprints on the other hand are contradicting and impossible
576 to fulfill. If the two EC towers are located in a distance large enough to ensure non
577 overlapping footprints, different environmental conditions at both EC towers can cause
578 systematic differences of the simultaneously measured fluxes that should not be included in
579 the uncertainty estimate. This study for the grassland site Rollesbroich in Germany showed
580 that the extended two-tower approach which includes a correction for systematic flux
581 differences (sfd-correction) can be used to derive more reliable (less overestimated)
582 uncertainty estimates compared to the classical two-tower approach. An advantage of this

583 extended two-tower approach is its simplicity and the fact that there is no need to quantify the
584 differences in environmental conditions (which is usually not possible due to a lack of data).
585 Comparing the uncertainty estimates for five different EC tower distances showed that the
586 mean uncertainty estimated with our extended two-tower approach for the 95 m and 173 m
587 distances were nearly identical to the random error estimated with the raw-data based
588 reference method. This suggests that these distances were most appropriate for the
589 application of the extended two-tower approach in this study. Also for the largest EC tower
590 distances (20.5 km, 34 km) the sfd-correction significantly improved the correlations of the
591 flux magnitude and the random error and significantly reduced the difference to the
592 independent, raw data based reference value. We therefore conclude that if no second EC
593 tower is available at a closer distance (but available further away), a rough, probably
594 overestimated *NEE* uncertainty estimate can be acquired with the extended two-tower
595 approach although environmental conditions at the two sites are not identical.

596 A statement about the transferability of our experiment to other sites and EC tower distances
597 requires further experiments. However, we assume transferability is given if both EC towers
598 are located at sites of the same vegetation type (e.g. C3-grasses, C4-crops, deciduous forest,
599 coniferous forest, etc.). Flux differences caused by a different phenology can be very hard to
600 separate from the random error estimate, even though they are expected to be mainly
601 systematic and could therefore be partly captured with the sfd-correction. Moreover, the EC
602 raw data should be processed in the same way (as done here) and the measurement devices
603 should be identical and installed at about the same measurement height. Important is also that
604 the instruments are calibrated thoroughly and consistently. Because this was true for the three
605 EC towers included in this study, we conclude that systematic flux differences that are
606 corrected for with the sfd-correction arise mainly from different environmental conditions

607 whereas calibration errors are assumed to have a very minor effect. Different weather
608 conditions at both EC tower sites are a main drawback for applications of the two-tower
609 approach. While systematic differences of the weather conditions are expected to be captured
610 by the sfd-correction, less systematic weather fluctuations e.g. related to cloud movement, are
611 difficult to be filtered of the two-tower based uncertainty estimate. Applying very strict
612 thresholds can lead to a too small dataset, especially if the measurement periods are short. If
613 EC raw data is available, we recommend to use an uncertainty estimation scheme like the one
614 presented in Mauder et al. (2013).

615 Appendix A

616 Tab. A1

617 *Summary of the 95% confidence intervals for the linear regression coefficients of the NEE*
618 *magnitudes - standard error relationships determined with Eq.1 for the four two two-tower based*
619 *correction schemes and the five EC tower distances*

Variables:	Two towers:	m	m _{lower}	m _{upper}	b	b _{lower}	b _{upper}
NEE_{negative} / $\sigma(\delta)$	EC1 / EC2 (8 m)	-0.012	-0.041	0.017	0.691	0.442	0.940
	EC1 / EC2 (95 m)	-0.045	-0.099	0.010	1.163	0.680	1.647
	EC1 / EC2 (173 m)	-0.052	-0.067	-0.036	1.747	1.537	1.957
	EC1 / EC2 (20.5 km)	-0.088	-0.272	0.097	2.544	0.696	4.392
	EC1 / EC3 (34 km)	-0.130	-0.330	0.069	2.849	0.772	4.926
NEE_{negative} / $\sigma(\delta)_f$	EC1 / EC2 (8 m)	-0.008	-0.043	0.026	0.746	0.497	0.995
	EC1 / EC2 (95 m)	-0.005	-0.036	0.026	1.569	1.286	1.853
	EC1 / EC2 (173 m)	-0.055	-0.088	-0.021	1.416	1.009	1.824
	EC1 / EC2 (20.5 km)	-0.011	-0.087	0.066	2.606	1.929	3.284
	EC1 / EC3 (34 km)	-0.039	-0.190	0.113	3.527	1.737	5.317
NEE_{negative} / $\sigma(\delta)_{corr}$	EC1 / EC2 (8 m)	-0.036	-0.048	-0.024	0.227	0.125	0.329
	EC1 / EC2 (95 m)	-0.043	-0.072	-0.014	0.699	0.379	1.018
	EC1 / EC2 (173 m)	-0.052	-0.087	-0.017	0.485	-0.059	1.030
	EC1 / EC2 (20.5 km)	-0.085	-0.142	-0.028	1.033	0.312	1.754
	EC1 / EC3 (34 km)	-0.092	-0.129	-0.055	0.963	0.421	1.505
NEE_{negative} / $\sigma(\delta)_{corr,f}$	EC1 / EC2 (8 m)	-0.040	-0.060	-0.019	0.211	0.053	0.369
	EC1 / EC2 (95 m)	-0.044	-0.074	-0.013	0.574	0.252	0.895
	EC1 / EC2 (173 m)	-0.071	-0.122	-0.021	0.272	-0.440	0.983
	EC1 / EC2 (20.5 km)	-0.106	-0.204	-0.009	0.493	-0.685	1.671
	EC1 / EC3 (34 km)	-0.070	-0.108	-0.031	0.981	0.346	1.616
NEE_{positive} / $\sigma(\delta)$	EC1 / EC2 (8 m)	0.101	0.027	0.174	0.346	-0.024	0.715
	EC1 / EC2 (95 m)	0.161	0.028	0.294	0.734	0.285	1.183
	EC1 / EC2 (173 m)	0.061	-0.284	0.406	1.340	-0.775	3.455
	EC1 / EC2 (20.5 km)	0.118	-0.272	0.507	1.332	-0.500	3.164
	EC1 / EC3 (34 km)	0.235	0.113	0.356	0.731	0.323	1.140
NEE_{positive} /	EC1 / EC2 (8 m)	0.101	0.020	0.182	0.340	-0.080	0.760

$\sigma(\delta)_f$	EC1 / EC2 (95 m)	0.029	-0.299	0.357	1.333	-0.114	2.780
	EC1 / EC2 (173 m)	0.179	-0.122	0.480	0.535	-1.316	2.385
	EC1 / EC2 (20.5 km)	0.145	-0.174	0.464	1.134	-0.365	2.632
	EC1 / EC3 (34 km)	0.320	0.059	0.580	0.763	-0.330	1.857
$\text{NEE}_{\text{positive}} / \sigma(\delta)_{\text{corr}}$	EC1 / EC2 (8 m)	0.083	0.043	0.123	0.089	-0.106	0.284
	EC1 / EC2 (95 m)	0.074	0.054	0.094	0.165	0.094	0.236
	EC1 / EC2 (173 m)	0.172	-0.093	0.436	-0.110	-1.979	1.759
	EC1 / EC2 (20.5 km)	0.245	0.122	0.367	-0.328	-0.938	0.282
	EC1 / EC3 (34 km)	0.162	0.135	0.189	0.080	-0.015	0.175
$\text{NEE}_{\text{positive}} / \sigma(\delta)_{\text{corr},f}$	EC1 / EC2 (8 m)	0.078	0.037	0.118	0.101	-0.102	0.303
	EC1 / EC2 (95 m)	0.090	0.030	0.150	0.136	-0.142	0.414
	EC1 / EC2 (173 m)	0.163	-0.132	0.459	-0.040	-2.081	2.000
	EC1 / EC2 (20.5 km)	0.159	-0.094	0.413	0.072	-1.205	1.349
	EC1 / EC3 (34 km)	0.205	0.132	0.279	0.029	-0.278	0.337

* m_{lower} , m_{upper} : lower and upper 95% confidence interval for slope m

* b_{lower} , b_{upper} : lower and upper 95% confidence interval for intersect b

$\sigma(\delta)$, $\sigma(\delta)_f$: uncertainty estimated with classical two-tower approach without & with weather filter (f)

$\sigma(\delta)_{\text{corr}}$, $\sigma(\delta)_{\text{corr},f}$: uncertainty estimated with extended two-tower approach

Tab. A2: R^2 for NEE uncertainty determined with the extended two-tower approach (including sfd-correction and weather-filter) as function of NEE_{corr} magnitude and for 20.5km EC tower distance. Results are given for different moving average time intervals (6 hr, 12 hr, 24hr) and data coverage percentages (25%, 50%, 70%) for the calculation of the sfd-correction factor (Eq.2)

	6h	12h	24h
30%	0.73; 0.84; (937)	0.92; 0.72; (904)	0.84; 0.82; (597)
50%	0.58; 0.85; (710)	0.7; 0.43; (463)	-; -; (32)
70%	0.77; 0.78; (408)	0.66; 0.08; (148)	-; -; (0)

black: for negative NEE; grey: for positive NEE; (): total number of half-hourly NEE left after sfd-correction and weather filter to build bins for NEE uncertainty versus NEE magnitude regressions (Fig.5 for 12h & 50 %)

620

621 **Tab. A3: Relative difference [%] of mean uncertainty $\sigma(\delta)_{\text{corr},f}$ estimated with the extended two**
622 **tower approach and the reference σ_{cov} for EC tower distances > 8m**

Diff	$\Delta\sigma_{\text{cov}}$ (6h)	$\Delta\sigma_{\text{cov}}$ (12h)	$\Delta\sigma_{\text{cov}}$ (24h)
30%	-0.8; 39.3	4.8; 55.5	10.9; 59.9
50%	-9.3; 32.5	-1.5; 41.2	-
70%	-10.5; 24.3	-5.2; 10.2	-

623 black: mean $\Delta\sigma_{\text{cov}}$ for 95m and 173m distance ; grey: mean $\Delta\sigma_{\text{cov}}$ for 20.5 km and 34 km distance

624

625

626

627 **Acknowledgments.** We are grateful to ExpeER (Experimentation in Ecosystem Research)
628 for funding this work. The eddy covariance data were provided by TERENO and the
629 Transregional Collaborative Research Centre 32 (TR32). We also thank Wittaya Kessomkiat
630 for his support. Moreover, we thank Qu Wei for providing the SoilNet data and Henning
631 Schiedung for providing the soil carbon and soil density data for the Rollesbroich site.

632 **References**

- 633 Allard, V., Soussana, J.-F., Falcimagne, R., Berbigier, P., Bonnefond, J.M., Ceschia, E.,
634 D'hour, P., Hénault, C., Laville, P., Martin, C., Pinarès-Patino, C., 2007. The role of
635 grazing management for the net biome productivity and greenhouse gas budget (CO₂,
636 N₂O and CH₄) of semi-natural grassland. *Agriculture, Ecosystems & Environment*
637 121, 47–58. doi:10.1016/j.agee.2006.12.004
- 638 Ammann, C., Flechard, C.R., Leifeld, J., Neftel, A., Fuhrer, J., 2007. The carbon budget of
639 newly established temperate grassland depends on management intensity. *Agriculture,*
640 *Ecosystems & Environment* 121, 5–20. doi:10.1016/j.agee.2006.12.002
- 641 Arbeitsgruppe BK50, 2001. Allgemeine Informationen zur Bodenkarte 1 : 50 000. - 55 S. ;
642 Krefeld (Geol. Dienst Nordrh.-Westf.).
- 643 Aubinet, M., Vesala, T., Papale, D., 2011. *Eddy Covariance: A Practical Guide to*
644 *Measurement and Data Analysis.* Springer Verlag.
- 645 Baldocchi, D.D., 2001. Assessing ecosystem carbon balance: problems and prospects of the
646 eddy covariance technique. *Annual Review of Ecology and Systematics* 33, 1–33.
- 647 Baldocchi, D.D., 2003. Assessing the eddy covariance technique for evaluating carbon
648 dioxide exchange rates of ecosystems: past, present and future. *Global Change*
649 *Biology* 9, 479–492.
- 650 Barr, A.G., Morgenstern, K., Black, T.A., McCaughey, J.H., Nesic, Z., 2006. Surface energy
651 balance closure by the eddy-covariance method above three boreal forest stands and
652 implications for the measurement of the CO₂ flux. *Agricultural and Forest*
653 *Meteorology* 140, 322–337. doi:10.1016/j.agrformet.2006.08.007
- 654 Billesbach, D.P., 2011. Estimating uncertainties in individual eddy covariance flux
655 measurements: A comparison of methods and a proposed new method. *Agricultural*
656 *and Forest Meteorology* 151, 394–405. doi:10.1016/j.agrformet.2010.12.001
- 657 Bogaena, H.R., Huisman, J.A., Meier, H., Rosenbaum, U., Weuthen, A., 2009. Hybrid
658 Wireless Underground Sensor Networks: Quantification of Signal Attenuation in Soil.
659 *Vadose Zone Journal* 8, 755–761. doi:10.2136/vzj2008.0138

- 660 Braswell, B.H., Sacks, W.J., Linder, E., Schimel, D.S., 2005. Estimating diurnal to annual
661 ecosystem parameters by synthesis of a carbon flux model with eddy covariance net
662 ecosystem exchange observations. *Global Change Biology* 11, 335–355.
663 doi:10.1111/j.1365-2486.2005.00897.x
- 664 Dragoni, D., Schmid, H.P., Grimmond, C.S.B., Loescher, H.W., 2007. Uncertainty of annual
665 net ecosystem productivity estimated using eddy covariance flux measurements.
666 *Journal of Geophysical Research-Atmospheres* 112, 1–9. doi:10.1029/2006JD008149
- 667 Finkelstein, P.L., Sims, P.F., 2001. Sampling error in eddy correlation flux measurements.
668 *Journal of Geophysical Research: Atmospheres* 106, 3503–3509.
669 doi:10.1029/2000JD900731
- 670 Flanagan, L.B., Johnson, B.G., 2005. Interacting effects of temperature, soil moisture and
671 plant biomass production on ecosystem respiration in a northern temperate grassland.
672 *Agricultural and Forest Meteorology* 130, 237–253.
673 doi:10.1016/j.agrformet.2005.04.002
- 674 Foken, T., Wichura, B., 1996. Tools for quality assessment of surface-based flux
675 measurements. *Agricultural and Forest Meteorology* 78, 83–105.
- 676 Goulden, M.L., Munger, J.W., Fan, S.M., Daube, B.C., Wofsy, S.C., 1996. Measurements of
677 carbon sequestration by long-term eddy covariance: Methods and a critical evaluation
678 of accuracy. *Global Change Biology* 2, 169–182.
- 679 Herbst, M., Prolingheuer, N., Graf, A., Huisman, J.A., Weihermüller, L., Vanderborght, J.,
680 2009. Characterization and Understanding of Bare Soil Respiration Spatial Variability
681 at Plot Scale. *Vadose Zone Journal* 8, 762. doi:10.2136/vzj2008.0068
- 682 Hill, T.C., Ryan, E., Williams, M., 2012. The use of CO₂ flux time series for parameter and
683 carbon stock estimation in carbon cycle research. *Global Change Biology* 18, 179–
684 193. doi:10.1111/j.1365-2486.2011.02511.x
- 685 Hollinger, D.Y., Aber, J., Dail, B., Davidson, E.A., Goltz, S.M., Hughes, H., Leclerc, M.Y.,
686 Lee, J.T., Richardson, A.D., Rodrigues, C., Scott, N. a., Achuatavarier, D., Walsh, J.,
687 2004. Spatial and temporal variability in forest–atmosphere CO₂ exchange. *Global
688 Change Biology* 10, 1689–1706. doi:10.1111/j.1365-2486.2004.00847.x
- 689 Hollinger, D.Y., Richardson, A.D., 2005. Uncertainty in eddy covariance measurements and
690 its application to physiological models. *Tree Physiology* 25, 873–885.
- 691 Kessomkiat, W., Hendricks-Franssen, H.-J., Graf, A., Vereecken, H., 2013. Estimating
692 random errors of eddy covariance data: An extended two-tower approach.
693 *Agricultural and Forest Meteorology* 171, 203–219.
- 694 Kormann, R., Meixner, F.X., 2001. An Analytical Footprint Model For Non-Neutral
695 Stratification. *Boundary-Layer Meteorology* 99, 207–224.
696 doi:10.1023/A:1018991015119

- 697 Korres, W., Koyama, C.N., Fiener, P., Schneider, K., 2010. Analysis of surface soil moisture
698 patterns in agricultural landscapes using Empirical Orthogonal Functions. *Hydrol.*
699 *Earth Syst. Sci.* 14, 751–764. doi:10.5194/hess-14-751-2010
- 700 Kuppel, S., Peylin, P., Chevallier, F., Bacour, C., Maignan, F., Richardson, A.D., 2012.
701 Constraining a global ecosystem model with multi-site eddy-covariance data.
702 *Biogeosciences Discuss.* 9, 3317–3380. doi:10.5194/bgd-9-3317-2012
- 703 Liu, H., Randerson, J., Lindfors, J., Massman, W., Foken, T., 2006. Consequences of
704 Incomplete Surface Energy Balance Closure for CO₂ Fluxes from Open-Path
705 CO₂/H₂O Infrared Gas Analysers. *Boundary-Layer Meteorology* 120, 65–85.
706 doi:10.1007/s10546-005-9047-z
- 707 Lloyd, J., Taylor, J.A., 1994. On the Temperature Dependence of Soil Respiration.
708 *Functional Ecology* 8, 315. doi:10.2307/2389824
- 709 Mauder, M., Cuntz, M., Drüe, C., Graf, A., Rebmann, C., Schmid, H.P., Schmidt, M.,
710 Steinbrecher, R., 2013. A strategy for quality and uncertainty assessment of long-term
711 eddy-covariance measurements. *Agricultural and Forest Meteorology* 169, 122–135.
- 712 Mauder, M., Foken, T., 2011. Documentation and instruction manual of the Eddy covariance
713 software package TK3. Univ. Bayreuth, Abt. Mikrometeorologie.
- 714 Orchard, V.A., Cook, F.J., 1983. Relationship between soil respiration and soil moisture. *Soil*
715 *Biology and Biochemistry* 15, 447–453. doi:10.1016/0038-0717(83)90010-X
- 716 Oren, R., Hsieh, C.-I., Stoy, P., Albertson, J., Mccarthy, H.R., Harrell, P., Katul, G.G., 2006.
717 Estimating the uncertainty in annual net ecosystem carbon exchange: spatial variation
718 in turbulent fluxes and sampling errors in eddy-covariance measurements. *Global*
719 *Change Biology* 12, 883–896. doi:10.1111/j.1365-2486.2006.01131.x
- 720 Qu, W., Bogen, H.R., Huisman, J.A., Martinez, G., Pachepsky, Y.A., Vereecken, H., 2014.
721 Investigating the controls of hydraulic properties on spatial variability of soil water
722 with sensor network data and inverse modeling approach. *Vadose Zone Journal*.
- 723 Qu, W., Bogen, H.R., Huisman, J.A., Vereecken, H., 2013. Calibration of a Novel Low-Cost
724 Soil Water Content Sensor Based on a Ring Oscillator. *Vadose Zone Journal* 12, 1–
725 10. doi:10.2136/vzj2012.0139
- 726 Richardson, A.D., Aubinet, M., Barr, A.G., Hollinger, D.Y., Ibrom, A., Lasslop, G.,
727 Reichstein, M., 2012. Uncertainty Quantification. *Eddy Covariance. A Practical*
728 *Guide to Measurement and Data Analysis* 173–209.
- 729 Richardson, A.D., Hollinger, D.Y., Burba, G.G., Davis, K.J., Flanagan, L.B., Katul, G.G.,
730 William Munger, J., Ricciuto, D.M., Stoy, P.C., Suyker, A.E., Verma, S.B., Wofsy,
731 S.C., 2006. A multi-site analysis of random error in tower-based measurements of
732 carbon and energy fluxes. *Agricultural and Forest Meteorology* 136, 1–18.
733 doi:10.1016/j.agrformet.2006.01.007
- 734 Richardson, A.D., Mahecha, M.D., Falge, E., Kattge, J., Moffat, A.M., Papale, D.,
735 Reichstein, M., Stauch, V.J., Braswell, B.H., Churkina, G., Kruijt, B., Hollinger,

736 D.Y., 2008. Statistical properties of random CO₂ flux measurement uncertainty
737 inferred from model residuals. *Agricultural and Forest Meteorology* 148, 38–50.
738 doi:10.1016/j.agrformet.2007.09.001

739 Tsubo, M., Walker, S., 2005. Relationships between photosynthetically active radiation and
740 clearness index at Bloemfontein, South Africa. *Theoretical and applied climatology*
741 80, 17–25.

742 Webb, E.K., Pearman, G.I., Leuning, R., 1980. Correction of flux measurements for density
743 effects due to heat and water vapour transfer. *Quarterly Journal of the Royal*
744 *Meteorological Society* 106, 85–100.

745 Wilson, K., Goldstein, A., Falge, E., Aubinet, M., Baldocchi, D., Berbigier, P., Bernhofer, C.,
746 Ceulemans, R., Dolman, H., Field, C., Grelle, A., Ibrom, A., Law, B., Kowalski, A.,
747 Meyers, T., Moncrieff, J., Monson, R., Oechel, W., Tenhunen, J., Valentini, R.,
748 Verma, S., 2002. Energy balance closure at FLUXNET sites. *Agricultural and Forest*
749 *Meteorology* 113, 223–243. doi:10.1016/S0168-1923(02)00109-0

750 Xu, L., Baldocchi, D.D., Tang, J., 2004. How soil moisture, rain pulses, and growth alter the
751 response of ecosystem respiration to temperature. *Global Biogeochem. Cycles* 18,
752 GB4002. doi:10.1029/2004GB002281

753 Zacharias, S., Bogen, H., Samaniego, L., Mauder, M., Fuß, R., Pütz, T., Frenzel, M.,
754 Schwank, M., Baessler, C., Butterbach-Bahl, K., Bens, O., Borg, E., Brauer, A.,
755 Dietrich, P., Hajsek, I., Helle, G., Kiese, R., Kunstmann, H., Klotz, S., Munch, J.C.,
756 Papen, H., Priesack, E., Schmid, H.P., Steinbrecher, R., Rosenbaum, U., Teutsch, G.,
757 Vereecken, H., 2011. A Network of Terrestrial Environmental Observatories in
758 Germany. *Vadose Zone Journal* 10, 955–973. doi:10.2136/vzj2010.0139

759

760

761

762

763

764

765

766

767

768 **Table Captions**

769 Tab. 1. Measurement periods and locations of the permanent EC towers in Rollesbroich
770 (EC1) and Merzenhausen (EC3) and the roving station (EC2)

771 Tab. 2. Mean NEE uncertainty [$\mu\text{mol m}^{-2} \text{s}^{-1}$] for five EC tower distances estimated with the
772 classical two-tower approach, with and without including a weather-filter ($\sigma(\delta)$, $\sigma(\delta)_f$
773). and with the extended two-tower approach (sfd-correction), also with and without
774 including a weather-filter ($\sigma(\delta)_{\text{corr}}$, $\sigma(\delta)_{\text{corr},f}$). The table also provides the random error
775 σ_{cov} [$\mu\text{mol m}^{-2} \text{s}^{-1}$] estimated with the raw-data based reference method (Mauder et al.
776 2013).

777 **Figure Captions**

778 Fig. 1. Eddy covariance (EC) tower locations in the Rur-Catchment (center) including the
779 Rollesbroich test site (left), with the target areas defined for the footprint analysis

780 Fig. 2. NEE uncertainty $\sigma(\delta)$ determined with the classical two-tower approach as function of
781 the NEE flux magnitude for the EC tower distances 8m (a), 95m (b) , 173m (c),
782 20.5km (d) and 34km (e). (Dashed line: linear correlation not significant ($p>0.1$))

783 Fig. 3. NEE uncertainty $\sigma(\delta)$ determined with the classical two-tower approach as function of
784 the NEE flux magnitude including the application of the weather-filter for the EC
785 tower distances 8m (a), 95m (b) , 173m (c), 20.5km (d) and 34km (e). (Dashed line:
786 linear correlation not significant ($p>0.1$))

787 Fig. 4. Scatter of the NEE measured at EC1 (NEE_{EC1}) and NEE measured at a second tower
788 EC2/EC3 (NEE_{EC2}) for the uncorrected NEE (left) and the sfd-corrected NEE_{corr}
789 (right) for the EC tower distances 8m (a), 95m (b) , 173m (c), 20.5km (d) and 34km
790 (e)

791 Fig. 5. NEE uncertainty $\sigma(\delta)_{\text{corr}}$ determined with the extended two-tower approach as
792 function of sfd-corrected NEE_{corr} magnitude (Eq.2) for the EC tower distances 8m (a),
793 95m (b) , 173m (c), 20.5km (d) and 34km (e) (Dashed line: linear correlation not
794 significant ($p>0.1$))

795 Fig. 6. NEE uncertainty $\sigma(\delta)_{\text{corr}}$ determined with the extended two-tower approach as function
796 of sfd-corrected NEE_{corr} magnitude (Eq.2) including application of the weather-filter
797 for the EC tower distances 8m (a), 95m (b) , 173m (c), 20.5km (d) and 34km (e)
798 (Dashed line: linear correlation not significant ($p>0.1$))

799

800

801

802
803

Tab. 1. Measurement periods and locations of the permanent EC towers in Rollesbroich (EC1) and Merzenhausen (EC3) and the roving station (EC2)

	Coordinates	Sitename	Distance to EC1	Measurement period	alt. (m)
EC1	50.6219142 N / 6.3041256 E	Rollesbroich	–	13.05.2011 – 15.07.2013	514.7
EC2	50.6219012 N / 6.3040107 E 50.6219012 N / 6.3040107 E	Rollesbroich	8m	29.07.2011 – 06.10.2011 05.03.2013 – 15.05.2013	514.8
	50.6217990 N / 6.3027962 E 50.6210472 N / 6.3042120 E	Rollesbroich	95m	07.10.2011 – 15.05.2012 01.07.2013 – 15.07.2013	516.3 517.3
	50.6217290 N / 6.3016925 E	Rollesbroich	173m	24.05.2012 – 14.08.2012	517.1
	50.5027500 N / 6.5254170 E	Kall-Sistig	20.5 km	14.08.2012 – 01.11.2012 15.05.2013 – 01.07.2013	498.0
EC3	50.9297879 N / 6.2969924 E	Merzenhausen	34 km	10.05.2011– 16.07.2013	93.3

804

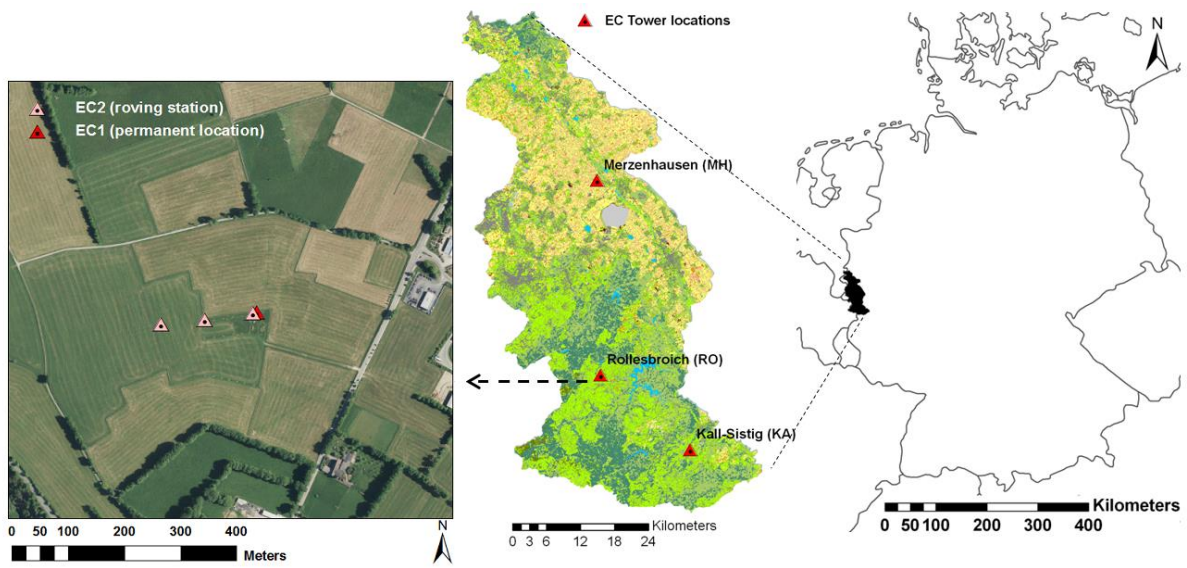
805
806
807
808
809
810

Tab. 2. Mean NEE uncertainty [$\mu\text{mol m}^{-2} \text{s}^{-1}$] for five EC tower distances estimated with the classical two-tower approach, with and without including a weather-filter ($\sigma(\delta)$, $\sigma(\delta)_f$). and with the extended two-tower approach (sfd-correction), also with and without including a weather-filter ($\sigma(\delta)_{\text{corr}}$, $\sigma(\delta)_{\text{corr},f}$). The table also provides the random error σ_{cov} [$\mu\text{mol m}^{-2} \text{s}^{-1}$] estimated with the raw-data based reference method (Mauder et al. 2013).

EC tower distance	N	$\sigma(\delta)$ ($\Delta\sigma_{\text{cov}}$)	$\sigma(\delta)_f$ ($\Delta\sigma_{\text{cov}}$)	$\sigma(\delta)_{\text{corr}}$ ($\Delta\sigma_{\text{cov}}$)	$\sigma(\delta)_{\text{corr},f}$ ($\Delta\sigma_{\text{cov}}$)	σ_{cov}
8m	3167	0.76 (18.8)	0.77 (20.5)	0.44 (-30.6)	0.44 (-30.8)	0.64
95m	3620	1.30 (116.7)	1.50 (149.4)	0.65 (8.2)	0.60 (0.2)	0.60
173m	2410	2.04 (98.5)	1.82 (77.0)	1.03 (-0.3)	1.00 (-2.5)	1.03
20.5 km	2574	2.72 (200.6)	2.35 (159.7)	1.52(67.8)	1.16 (28.7)	0.91
34 km	15571	2.73 (274.7)	2.86 (292.4)	1.18 (61.5)	1.14 (56.8)	0.73
mean		1.91	1.86	0.98	0.93	0.78

811
812

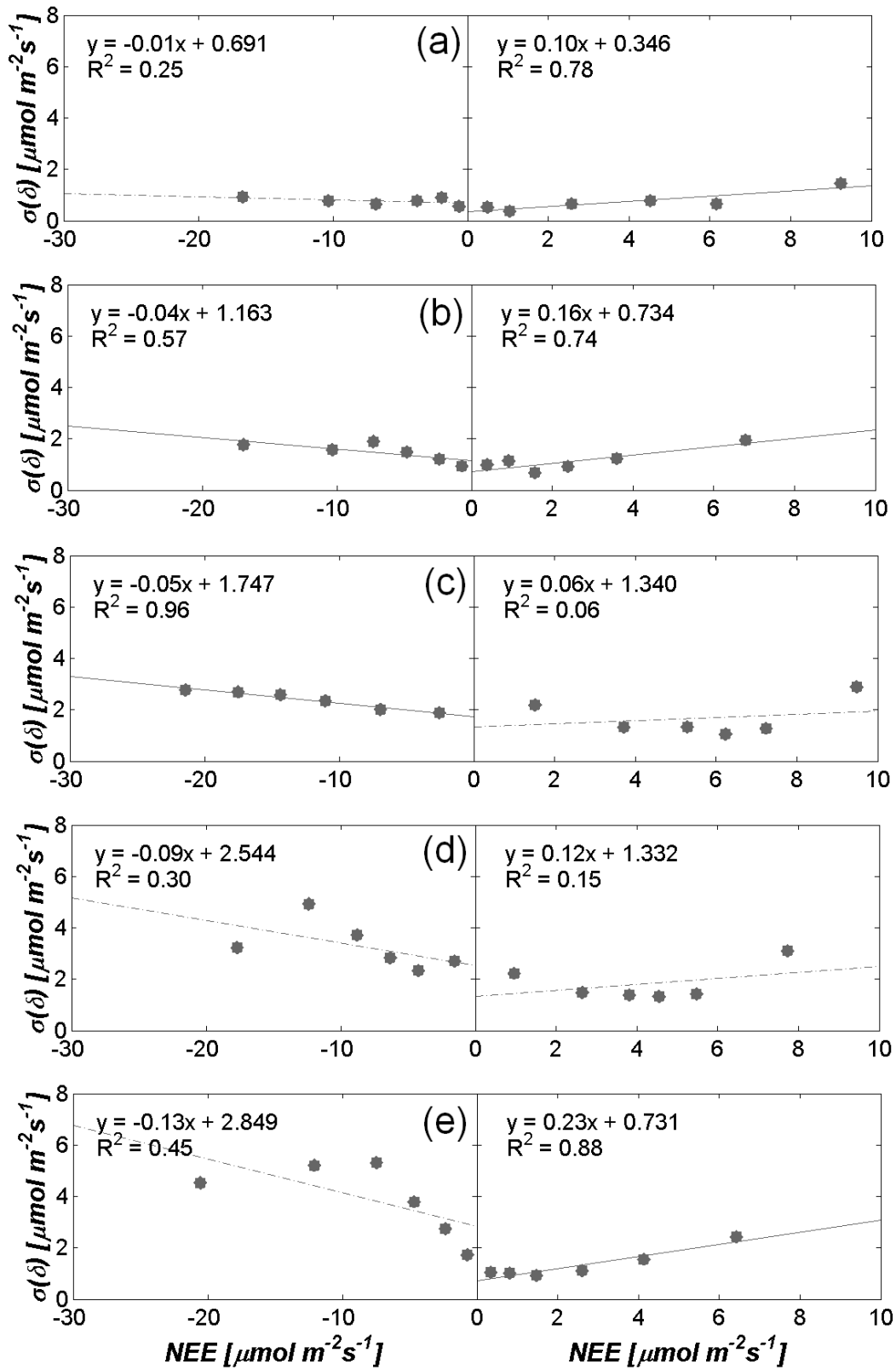
($\Delta\sigma_{\text{cov}}$): relative differences [%] between two-tower based uncertainty estimates and the references value σ_{cov} (Eq.4)



813

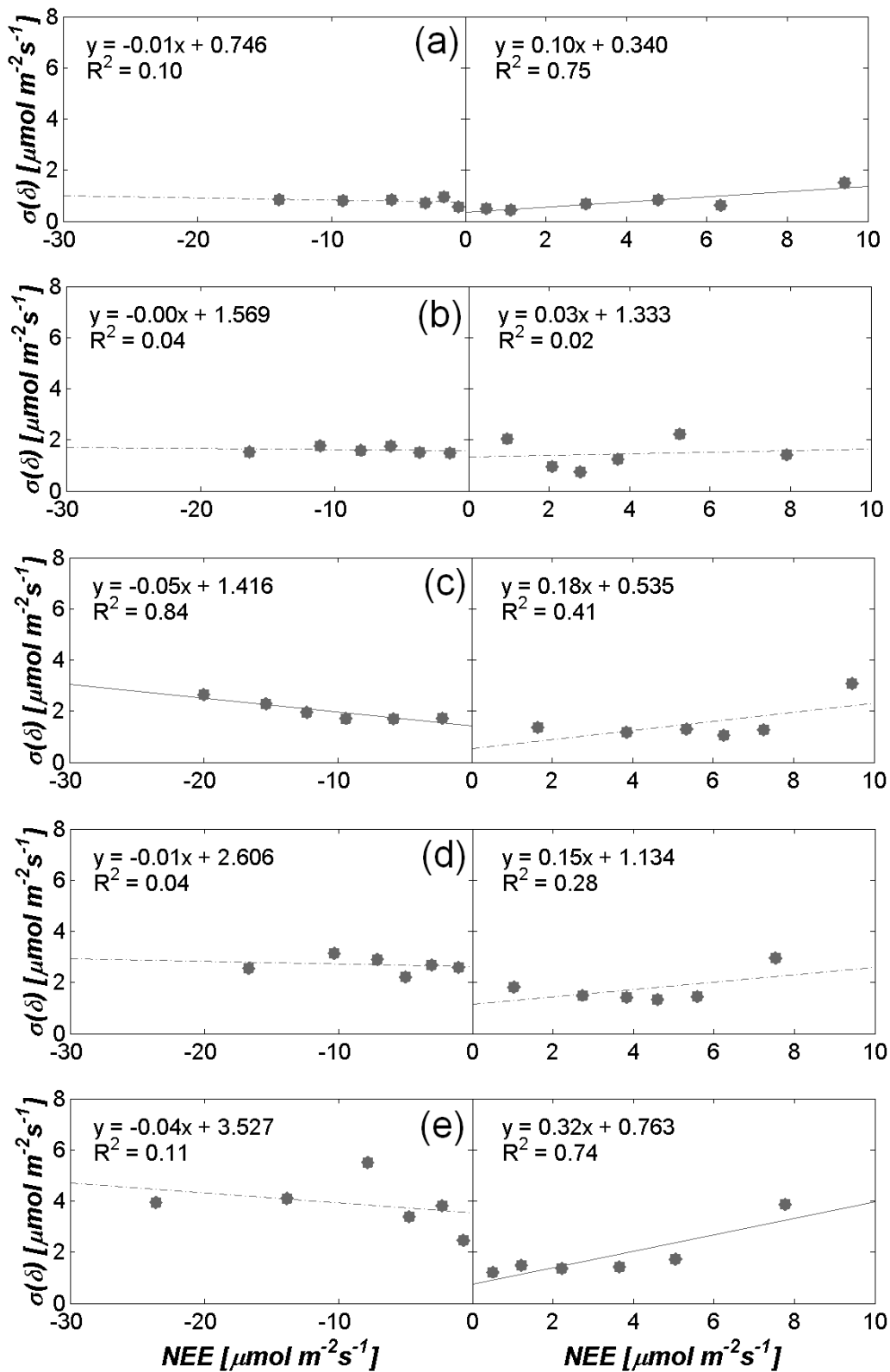
814 *Fig. 1. Eddy covariance (EC) tower locations in the Rur-Catchment (center) including the*
 815 *Rollesbroich test site (left)*

816



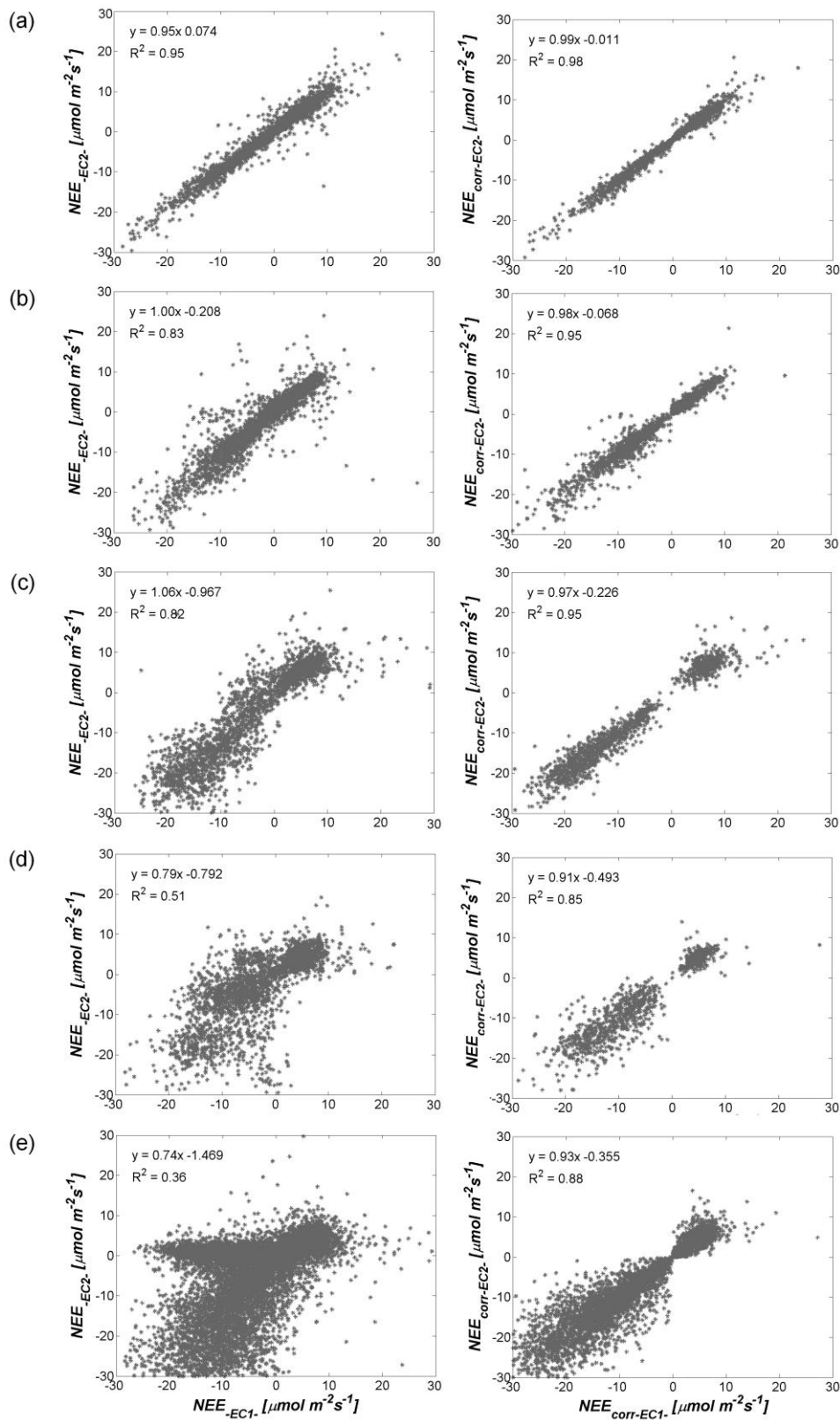
817

818 *Fig. 2. NEE uncertainty $\sigma(\delta)$ determined with the classical two-tower approach as function of the*
 819 *NEE flux magnitude for the EC tower distances 8m (a), 95m (b), 173m (c), 20.5km (d) and 34km*
 820 *(e). (Dashed line: regression slope not significantly different from zero ($p > 0.1$))*



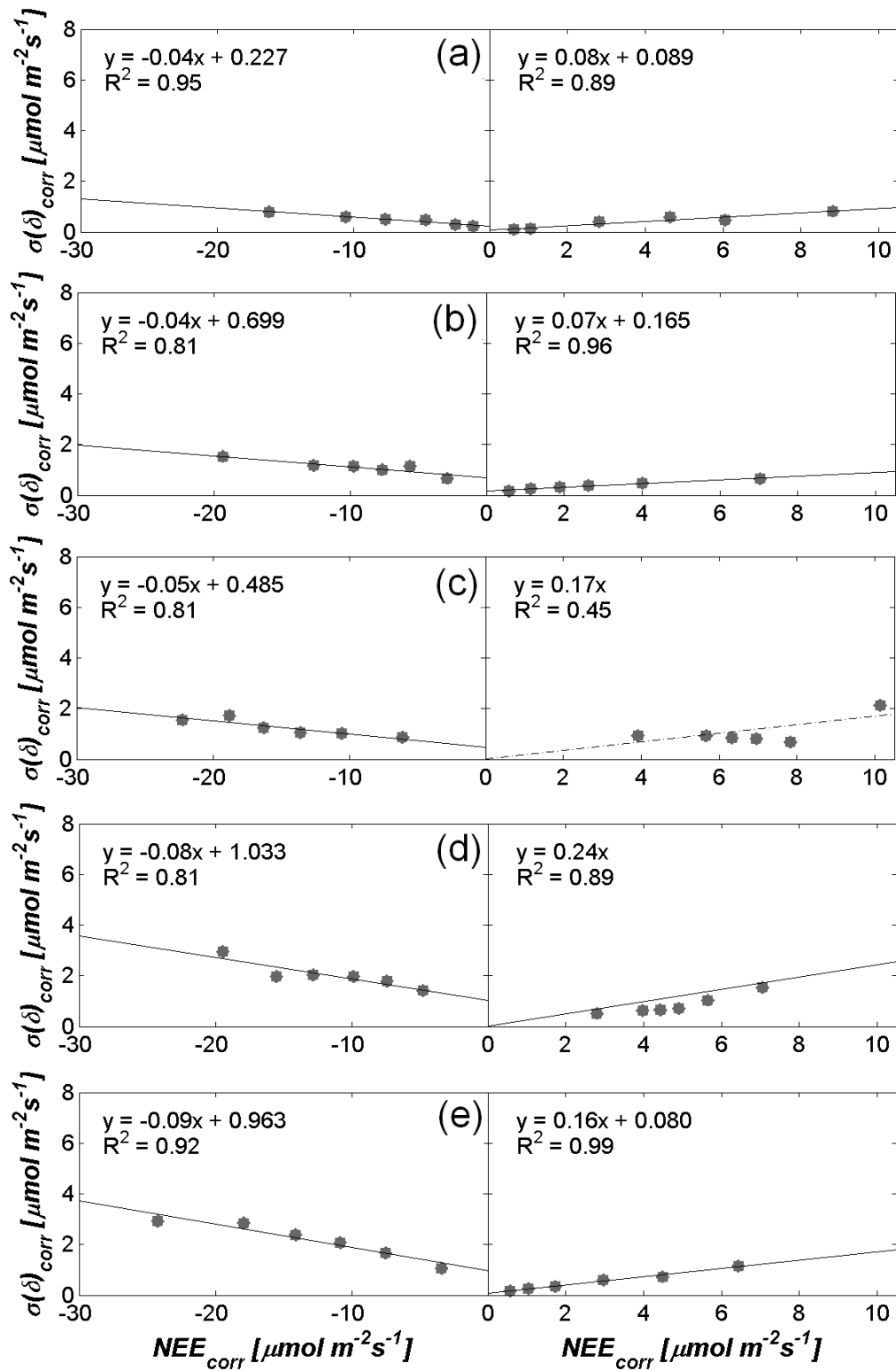
821

822 *Fig. 3. NEE uncertainty $\sigma(\delta)$ determined with the classical two-tower approach as function of the*
 823 *NEE flux magnitude including the application of the weather-filter for the EC tower distances 8m*
 824 *(a), 95m (b), 173m (c), 20.5km (d) and 34km (e). (Dashed line: regression slope not significantly*
 825 *different from zero ($p > 0.1$))*



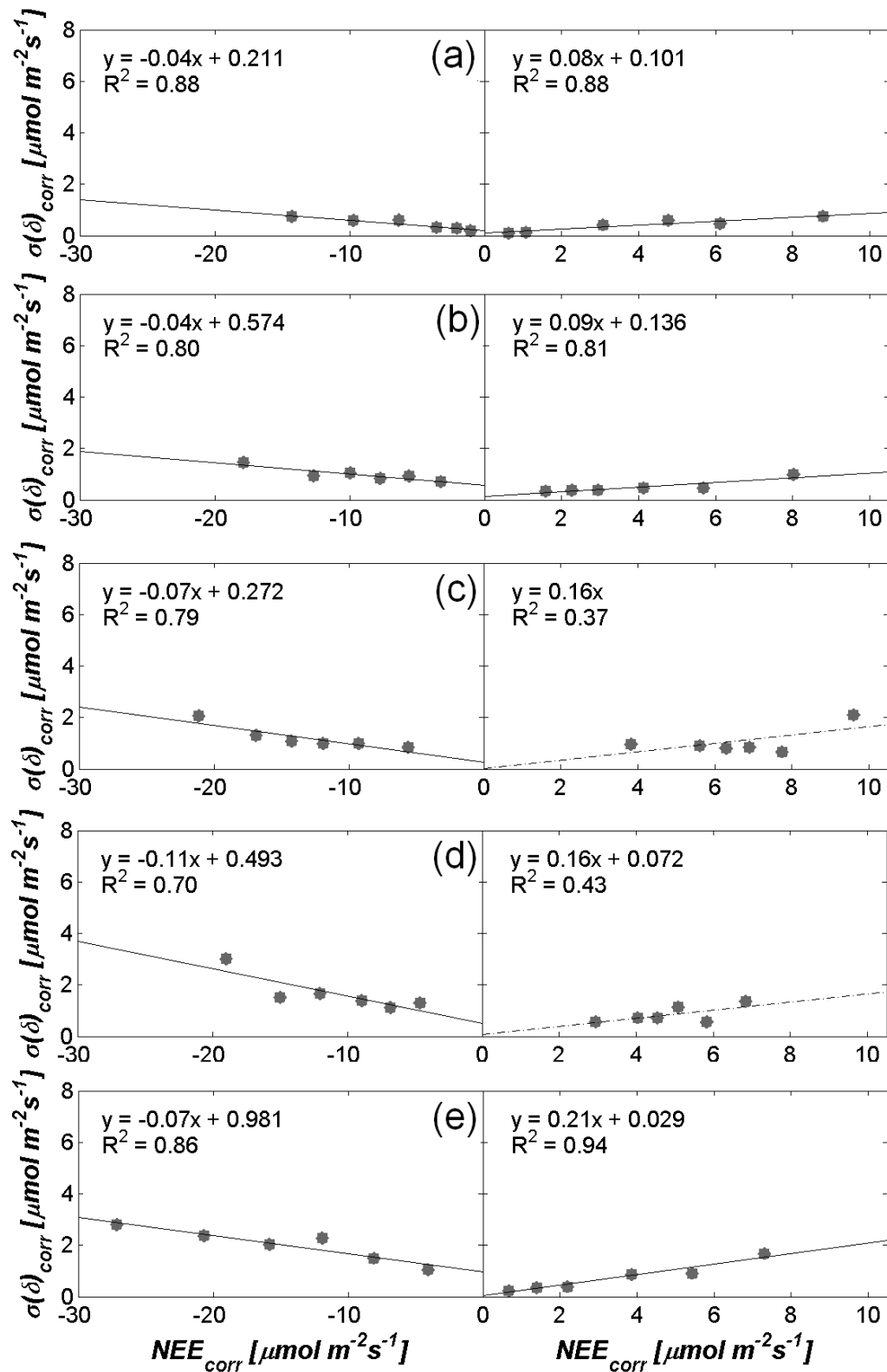
826

827 *Fig.4. Scatter of the NEE measured at EC1 (NEE_{-EC1}) and NEE measured at a second tower*
 828 *EC2/EC3 (NEE_{-EC2}) for the uncorrected NEE (left) and the sfd-corrected NEE_{corr} (right) for the*
 829 *EC tower distances 8m (a), 95m (b) , 173m (c), 20.5km (d) and 34 km*



830

831 *Fig.5. NEE uncertainty $\sigma(\delta)_{corr}$ determined with the extended two-tower approach as function of*
 832 *sfd-corrected NEE_{corr} magnitude (Eq.2) for the EC tower distances 8m (a), 95m (b), 173m (c),*
 833 *20.5km (d) and 34km (e) (Dashed line: regression slope not significantly different from zero*
 834 *($p > 0.1$))*



835

836 *Fig.6. NEE uncertainty $\sigma(\delta)_{corr}$ determined with the extended two-tower approach as function of*
 837 *sfd-corrected NEE_{corr} magnitude (Eq.2) including application of the weather-filter for the EC tower*
 838 *distances 8m (a), 95m (b) , 173m (c), 20.5km (d) and 34km (e) (Dashed line: regression slope not*
 839 *significantly different from zero ($p>0.1$))*